# A Multi-objective Trajectory Planning Scheme for Parallel Assembly Mechanism with B-spline Curves

Dong Chen, Shiqi Li, Junfeng Wang and Yi Feng
School of Mechanical Science & Engineering
Huazhong University of Science and Technology
Wuhan, China

Yang Liu
College of Engineering & Design
Hunan Normal University
Changsha, China

***Abstract*—An assembly mechanism based on the 6-UPU parallel manipulator is developed for the automated assembly of cabins. In this paper, the B-spline curves are employed to design the motion trajectories of the upper platform. The total motion time, energy consumption and the maximum absolute value of actuator's jerk are defined as three cost functions to evaluate the performance of trajectory. Artificial Immune Algorithm is used to solve the constrained multi-objective trajectory optimization problem. The trajectories of the actuators can also be obtained via the inverse kinematics model. The simulation results have confirmed that the proposed trajectory planning scheme is very effective to meet different requirements of pose adjustment.**

***Keywords—parallel assembly mechanism; automated assembly; trajectory planning; B-spline curve; multi-objective optimization***

## I. INTRODUCTION

The rapid development of aerospace industry has proposed higher demand for the performance and quality of spacecraft. Assembly operation of cabins or large-size components, always being considered as a key segment in the final assembly of spacecraft, has important influence on the accuracy, efficiency and quality of spacecraft. Now different kinds of automated assembly execution mechanisms, such as POGO stick with three-axis, numerical control brackets and parallel manipulators, are applied to accomplish the assembly operation [1] [2].

In recent years, parallel manipulators have been gradually implemented in accuracy assembly field due to the advantages of high rigidity, strong carrying capacity and small errors [3]. One of the prerequisites to make effective use of parallel manipulators is the proper trajectory planning of its end-effector. The purpose of trajectory planning is to obtain a continuous trajectory between two given poses for the end-effector [4]. In some practical applications, the planned trajectory must be optimized to satisfy different kinds of performance indexes as well as the kinematics and dynamics constraints provided by the structures [5][6].

In this paper, an assembly mechanism based on the 6-UPU parallel manipulator is developed for automated assembly of cabins. In order to get an accurate position and meet the requirements of various performance indexes at the same time, a multi-objective trajectory planning scheme based on B-spline curves has been proposed. Then the optimization model is calculated by Artificial Immune Algorithm (AIA). Finally, the trajectories of upper platform in Cartesian space and actuators in joint space all have been obtained.

## II. THE CABIN ASSEMBLY MECHANISM

### A. The Cabin Assembly Mechanism

The cabin assembly mechanism mainly consists of two parts: the upper flexible support platform and the lower parallel assembly platform, as is shown in Fig.1. The upper flexible support platform, designed to clamp and support the cabin in the process of pose adjustment, is mainly made up of clampers, accompanying fixture, flexible grippers and actuating structure. The lower parallel assembly platform (PAP) is designed basing on a 6-UPU parallel manipulator. It is also the core part to realize the pose adjustment of cabin.

The PAP mainly comprises a mobile platform, a static platform, and six electric cylinders. Each electric cylinder can be seen as two segments, the lower segment, a cylinder block, which connect with the static platform by universal joints, and the upper segment, a screw, which connect with the mobile platform by universal joints. The screw can move along the axis of the cylinder block actively and rotate around the axis passively when driven by the servo motor. The mobile platform will have a motion ability of 6-degree of freedom (6-DOF) in the workspace through the cooperative movements of six electric cylinders.

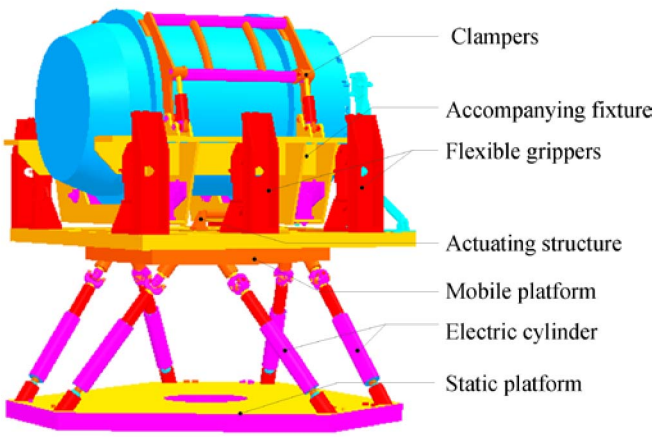


Fig. 1. The Cabin Assembly Mechanism

978-1-5386-5053-0/18/$31.00 ©2018 IEEE

*B. The kinematics analysis of PAP*

The trajectory of the upper platform to be planned is actually a reflection of its position and orientation information at every moment in the workspace. In order to get displacement, velocity and other physical information of the actuators, the inverse kinematics model of PAP should be established first [7].The simplified geometric structure and one of the six closed-loop chains of PAP are depicted in Fig.2.

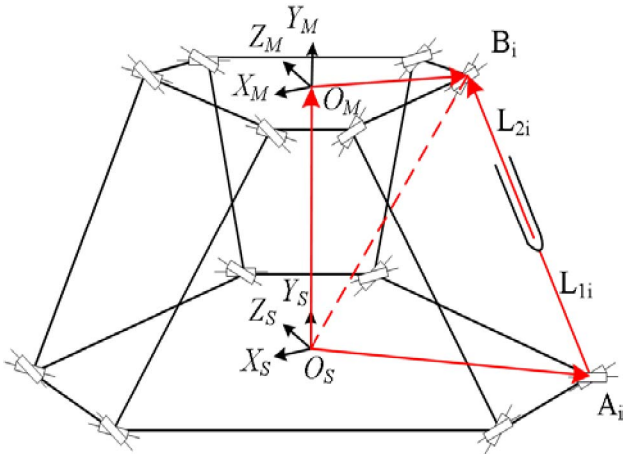


Fig. 2. The geometric structure and the closed-loop chain of PAP

Assuming that an inertia coordinate system $\{S\}$, $O_S$-$SxSySz$ is fixed to the static platform and frame $\{M\}$, $O_M$-$MxMyMz$ is attached to the gravity center of the upper platform. The pose of the upper platform can be expressed by the matrix $P=[{}^S_M R \quad {}^S_M T]^T$, in which ${}^S_M T$ denotes as the position vector $[x, y, z]^T$ of the upper platform with respect to the frame $\{S\}$, and the rotation matrix ${}^S_M R$ is defined by a set of Euler angles $[\alpha, \beta, \gamma]^T$ specifying the orientations of the upper platform. With the rotation sequence of ZYX, ${}^S_M R$ can be expressed as

$$
\begin{aligned}
{}^S_M R &= R_z(\alpha) R_y(\beta) R_x(\gamma) \\
&= \begin{bmatrix} c\alpha c\beta & c\alpha s\beta s\gamma - s\alpha c\gamma & c\alpha s\beta c\gamma + s\alpha s\gamma \\ s\alpha c\beta & s\alpha s\beta s\gamma + c\alpha c\gamma & s\alpha s\beta c\gamma - c\alpha s\gamma \\ -s\beta & c\beta s\gamma & c\beta c\gamma \end{bmatrix}
\end{aligned} \tag{1}
$$

Where c(.) and s(.) are short for cos(.) and sin(.).

The position vector of the upper universal joint $B_i$ and the lower universal joint $A_i$ with respect to the frame $\{S\}$ are respectively defined as $b_i$ and $A_i$. According to one of the closed-loop chains existing in the geometric structure, as is shown in Fig.2, the constraint equation of vector loop relation can be formulated as

$$
{}^S_M T + {}^S_M R B_i = A_i + L_i \tag{2}
$$

The length vector and the length magnitudes of the lower segment and the upper segment of the $i$-th link are respectively expressed as $L_{i1}$, $L_{i2}$ and $l_{i1}$, $l_{i2}$. $s_i$ is assumed as a unit vector along the $i$-th link in frame $\{S\}$, the inverse kinematics model of PAP can be obtained as

$$
(l_{i1} + l_{i2})\mathrm{s}_i = {}^S_M R B_i - A_i + {}^S_M T \tag{3}
$$

In (3), the pose vector of the upper platform can be abstracted out as the variables to the function of the length vector, then the inverse kinematics model can also be simply expressed as

$$
L_i = f_{inv}(x, y, z, \alpha, \beta, \gamma), (i = 1, 2, ..., 6) \tag{4}
$$

*C. The dynamics model of PAP*

Basing on the position and orientation information provided by the trajectory to be planned, It is essential to calculate the forces and torques produced by the actuators with the dynamics model of PAP. In this paper, the dynamics model of PAP is established basing on the virtual work approach [8], which can be formulated in terms of the Cartesian space coordinates as the following four equations

$$
J_M^T \tau_{act} + \tau_{ext} = M_t \ddot{x}_M + C_t \dot{x}_M + G_t \tag{5}
$$

$$
M_t = M_M + \sum_i J_i^T M_i J_i \tag{6}
$$

$$
C_t = C_M + \sum_i (J_i^T C_i J_i + J_i^T M_i \dot{J}_i) \tag{7}
$$

$$
G_t = G_M + \sum_i J_i^T G_i \tag{8}
$$

Where $J_M$ is the Jacobian matrix of the upper platform. $J_i$ is the Jacobian of $i$-th link. $\tau_{act}$ are the output force provided by the actuators. $\tau_{ext}$ are the external force and torque. $\ddot{x}_M$ and $\dot{x}_M$ are the acceleration and velocity vectors of the upper platform. $M_t$, $M_M$ and $M_i$ are the total mass matrix, the upper platform mass matrix and the link mass matrix. $C_t$, $C_M$ and $C_i$ are the total, the upper platform and the link Coriolis matrices. $G_t$ is the total gravity vectors includes $G_M$ and $G_i$, which are applied in the gravity center of the upper platform and each link respectively.

## III. The Multi-objective Trajectory Planning Scheme

The motion trajectory of upper platform and the kinematics and dynamics limitations are parameterized by the B-Spline curves [9]. Three cost functions have been defined as there performance indexes. Under the kinematics and dynamics constraints provided by the structures of PAP, the trajectory planning problem can be converted into a nonlinear constrained multi-objective optimization problem. Then AIA is used to solve the Pareto optimal solutions of B-Spline curve parameters. With these Pareto optimal parameters, the trajectory of upper platform is obtained and trajectories of actuators can also be acquired via the inverse kinematics model.

*A. Parameterized Representation of the Trajectories with B-spline Curves*

A B-Spline function of degree k with n+1 control points is defined as

$$p(u)=\sum_{i=0}^{n} d_i N_{i,k}(u) \tag{9}$$

$$\begin{cases} N_{i,0}(u)=\begin{cases}1, & u_i \le u < u_{i+1}\\ 0, & otherwise\end{cases} \\ N_{i,k}(u)=\dfrac{u-u_i}{u_{i+k}-u_i}N_{i,k-1}(u)+\dfrac{u_{i+k+1}-u}{u_{i+k+1}-u_{i+1}}N_{i+1,k-1}(u) \\ \dfrac{0}{0}=0 \end{cases}$$

For a fifth-order B-Spline curve with eleven control points, the trajectory of the upper platform at each time sub-interval can be interpolated as

$$P(t)=\sum_{i=0}^{10} d_i^P \cdot N_{i,5}(t) \tag{10}$$

The upper platform must start or stop its motion with zero linear velocity and acceleration from initial position to the final position, so the first and last control points of B-spline curve must be equal to the initial and final position vector of the upper platform

$$\begin{aligned} d_0 &= \left(d_0^1, d_0^2, d_0^3, d_0^4, d_0^5, d_0^6\right)^T = P_{ini} \\ d_{10} &= \left(d_9^1, d_9^2, d_9^3, d_9^4, d_9^5, d_9^6\right)^T = P_{fin} \end{aligned} \tag{11}$$

According to the properties of B-spline curve and the boundary conditions provided by (11), to generate a trajectory with zero initial and final velocity and acceleration, the following conditions on the control points of the trajectory should also be held

$$\begin{aligned} d_0 = d_1 = d_2 &= \left(P_{ini}^x, P_{ini}^y, P_{ini}^z, P_{ini}^\alpha, P_{ini}^\beta, P_{ini}^\gamma\right)^T \\ d_8 = d_9 = d_{10} &= \left(P_{fin}^x, P_{fin}^y, P_{fin}^z, P_{fin}^\alpha, P_{fin}^\beta, P_{fin}^\gamma\right)^T \end{aligned} \tag{12}$$

And the initial and final elements of the knot vector elements must be repeated six times as

$$\begin{aligned} t_i^P &= \{0,0,0,0,0,0,t_1,t_2,t_3,t_4,t_5,t_f,t_f,t_f,t_f,t_f,t_f\} \\ 0 &< t_1 \le t_2 \le t_3 \le t_4 \le t_5 < t_f \end{aligned} \tag{13}$$

A parameterized motion trajectory of the upper platform has been represented with equations from (10) to (13). It is obvious that the generalized coordinate values of five control points $\{d_3, d_4, d_5, d_6, d_7\}$ and the node vectors $\{t_1, t_2, t_3, t_4, t_5, t_f\}$ have become the unknown variables after simplification.

The velocity, acceleration and jerk trajectory of the upper platform can also be obtained by calculating the time derivatives of B-Spline function. According to the properties of B-spline curve, the velocity, acceleration and jerk of the upper platform are four, three and two order B-Spline curves that consist of ten, nine and eight control points respectively, in the following form

$$\begin{aligned} V(t) &= \sum_{i=0}^{n-1} d_i^V \cdot N_{i,k-1}(t) = \sum_{i=0}^{9} d_i^J \cdot N_{i,2}(t) \\ A(t) &= \sum_{i=0}^{n-2} d_i^A \cdot N_{i,k-2}(t) = \sum_{i=0}^{8} d_i^V \cdot N_{i,4}(t) \\ J(t) &= \sum_{i=0}^{n-3} d_i^J \cdot N_{i,k-3}(t) = \sum_{i=0}^{7} d_i^A \cdot N_{i,3}(t) \end{aligned} \tag{14}$$

Where the control points of velocity, acceleration and jerk are respectively calculated as

$$\begin{aligned} d_i^V &= \frac{k\cdot(d_{i+1}^P - d_i^P)}{t_{i+k+1}^P - t_{i+1}^P};\ (i=0,1,...,n-1) \\ d_i^A &= \frac{(k-1)\cdot(d_{i+1}^V - d_i^V)}{t_{i+k}^V - t_{i+1}^V};\ (i=0,1,...,n-2) \\ d_i^J &= \frac{(k-2)\cdot(d_{i+1}^A - d_i^A)}{t_{i+k-1}^A - t_{i+1}^A};\ (i=0,1,...,n-3) \end{aligned} \tag{15}$$

And the corresponding knot vector of velocity, acceleration and jerk are defined as

$$\begin{aligned} t_i^V &= \{0,0,0,0,0,t_1,t_2,t_3,t_4,t_5,t_f,t_f,t_f,t_f,t_f\} \\ t_i^A &= \{0,0,0,0,t_1,t_2,t_3,t_4,t_5,t_f,t_f,t_f,t_f\} \\ t_i^J &= \{0,0,0,t_1,t_2,t_3,t_4,t_5,t_f,t_f,t_f\} \end{aligned} \tag{16}$$

Based on the aforementioned trajectories of the upper platform, the displacement, velocity, acceleration and jerk curves of actuated links can also be formulated in terms of the control points and knot vector elements of B-Spline trajectory via the inverse kinematics model.

*B. The Multi-objective Trajectory Optimization Model*

In order to evaluate the planned trajectory, three important performance indexes i.e. the total motion time of cabin, the energy consumption of PAP and the maximum absolute value of actuators' jerk have been defined as three cost functions. Under the constraints imposed by the structure of PAP, the trajectory planning problem can be converted into a constrained multi-objective optimization problem.

The kinematic constraints are mainly the leg length limits, the linear velocities, accelerations and jerks limits of the actuators. The dynamic constraints are mainly the forces and

torques limitations of the actuators. Then a multi-objective trajectory optimization model can be expressed as

$$\begin{aligned}
&\min\ F(x) = (f_1(x), f_2(x), f_3(x)) \\
&\quad f_1(x) = t_{totle} = \int_0^{t_f} 1dt \\
&\quad f_2(x) = E = \int_0^{t_f} \left|\tau_{\text{act}} \cdot V_{\text{act}}(t)\right| dt \\
&\quad f_3(x) = \left|J_{act}^{\max}\right| = \max\left| f_{inv}(\sum_{i=0}^{7} d_i^J \cdot N_{i,2}(t))\right| \qquad (17) \\
&s.t.:\ \left|L_i(P)\right| \le L_{\max} \\
&\quad \left|\dot{L}_i(P,\dot{P})\right| \le \dot{L}_{\max} \\
&\quad \left|\ddot{L}_i(P,\dot{P},\ddot{P})\right| \le \ddot{L}_{\max} \\
&\quad \left|\dddot{L}_i(P,\dot{P},\ddot{P},\dddot{P})\right| \le \dddot{L}_{\max},\ (i = 1,2,...,6)
\end{aligned}$$

### C. Trajectory optimization with the AIA

The Artificial Immune Algorithm (AIA) is a useful tool to solve complicated nonlinear optimization problems [10]. For the aforementioned multi-objective trajectory optimization model, the three objective functions can be considered as the antigens and the variables of B-spline curve as the antibodies. These antibodies are also the solutions to the optimization problem, and updated through the action of clonal selected, crossover and mutation.

The main calculation procedure of AIA is expressed as the following seven steps

- Binary coding of antibodies and initialization to generate an initial group assumed as $A_0$.
- Calculate the affinity between each antibody and the three antigens, and meanwhile check the constraints.
- Determine the degree of dominated antibody for the current generation. The $A_0$ will be divided into two sub-generations, the non-Pareto optimization solution set $A_0^n$ and the Pareto optimization solution set $A_0^*$. Loop the following steps if the maximum number of iterations is not reach.
- Calculate the similarity and concentration of antibodies, clone the $A_0^*$ into memory cells to construct a memory set. Meanwhile, delete the duplicate and some dense antibodies in memory cells.
- Calculate the expected reproduction rate of antibodies, the antibodies with a higher rate will be cloned and selected.
- Antibodies crossover and elitist crossover are conducted with proper crossover probabilities.
- Antibodies mutation, then renew the antibodies.

## IV. THE NUMERICAL SIMULATION

To obtain the optimal trajectory of the upper platform, the previous described trajectory planning scheme has been implemented in MATLAB software.

### A. Configuration of the Parameters

The initial pose of the upper platform in Cartesian space is assumed as $P_{ini}=[0, 1005.07, 0, 0, 0, 0]^T$, and the final pose is assumed as $P_{fin}=[103.26, 1028.47, -6.18, 4.36°, -2.58°, 3.24°]^T$. The lower bounds and upper bounds of each control point have the same value with initial and final pose, respectively (i.e. $L_b=P_{ini}, L_u=P_{fin}$). The boundary of each time nodes is [0.1, 60].

The kinematics parameters of PAP and the constraint conditions have been listed in Table 1 and Table 2, respectively. Note that the coordinate value of $A_i$ and $B_i$ are in the frame $\{S\}$ and $\{M\}$, respectively. The mass of the upper platform is 447.92kg, and the mass of each actuator is 99.12kg for its lower segment and 17.99kg for its upper segment.

TABLE I. KINEMATICS PARAMETERS OF THE PAP

| Joint point | Coordinate value [mm] | | |
|---|---|---|---|
| | X | Y | Z |
| A1 | -512.65 | 0.00 | 1408.31 |
| A2 | -963.58 | 0.00 | 1147.96 |
| A3 | -963.58 | 0.00 | -1147.96 |
| A4 | -512.65 | 0.00 | -1408.31 |
| A5 | 1475.69 | 0.00 | -260.35 |
| A6 | 1475.69 | 0.00 | 260.35 |
| B1 | 239.78 | -233.70 | 658.12 |
| B2 | -689.86 | -233.70 | 121.42 |
| B3 | -689.86 | -233.70 | -121.42 |
| B4 | 239.78 | -233.70 | -658.12 |
| B5 | 450.08 | -233.70 | -536.70 |
| B6 | 450.08 | -233.70 | 536.70 |

TABLE II. LIMITATIONS OF THE ACTUATORS

| Displacement Limit (mm) | Velocity Limit (mm/s) | Acceleration Limit(mm/s2) | Jerk Limit (mm/s3) | Force Limit (N) |
|---|---|---|---|---|
| 250 | 15 | 20 | 150 | 3500 |

In the process of multi-objective trajectory optimization, the initial population size of antibody is 180, the cross probability is 0.8 and mutation probability is 0.2. To increase the diversity of solutions, the threshold of the allelic similarity of antibody is set as 0.6. To get a better evenness of solutions, the screening threshold of antibody is set as 0.1.

### B. Results and discussion

TABLE III. THE PARETO OPTIMAL SOLUTIONS

| Sol. Num. | $t_{total}$ (s) | E (J) | $\left\|J_{act}^{\max}\right\|$ (mm/s3) |
|---|---|---|---|
| 1 | **13.2290** | 590.9442 | 80.2547 |
| 2 | 41.8716 | **534.9809** | 0.4507 |
| 3 | 58.1619 | 627.8426 | **0.0710** |
| 4 | 32.8239 | 539.8275 | 0.8165 |
| 5 | 20.4133 | 560.6964 | 2.3507 |
| 6 | 17.7856 | 559.5589 | 5.1738 |
| 7 | 18.2296 | 546.5203 | 7.4551 |
| 8 | 17.1669 | 543.2831 | 27.6839 |
| 9 | 16.7738 | 550.7996 | 56.2927 |
| 10 | 13.9860 | 587.5719 | 72.6191 |

A total of 223 groups of Pareto solutions have been obtained by AIA under 500 iterations. The distribution of total Pareto optimal front are shown in Fig.3. Ten groups of optimal results of each cost functions have been listed in the 1st, 2nd and 3rd rows of Table 3.

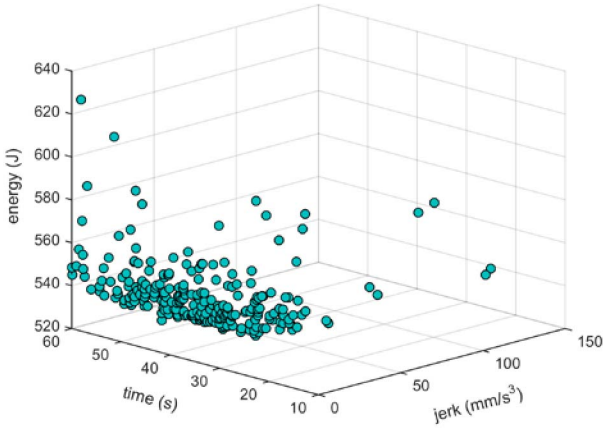


Fig. 3. The distribution of Pareto optimal front

Then the position and orientation trajectories of the upper platform in three optimal situations are depicted in Fig.4 and Fig.5, respectively. In order to make the results more intuitive, the decomposed motion trajectories of the upper platform in the situation of three directions and three angles have also been depicted in Fig.6. The displacement and jerk curves of actuated links are obtained via the inverse kinematics model. These optimal solutions in minimum total motion time, minimum maximum absolute value of actuator's jerk and minimum energy consumption are depicted in Fig.7-9.

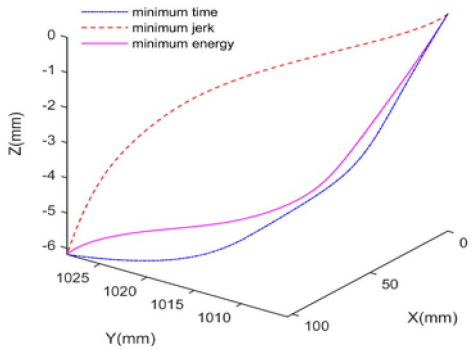


Fig. 4. The position trajectories of the upper platform

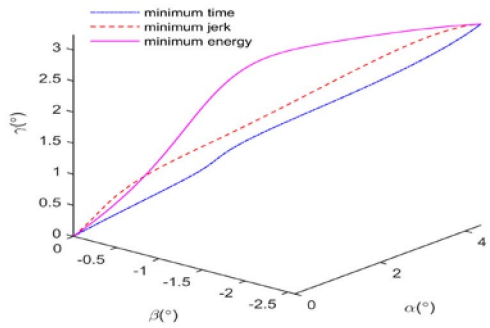


Fig. 5. The orientation trajectories of the upper platform

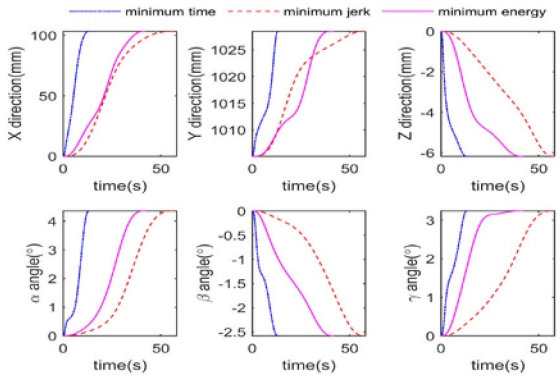


Fig. 6. The decomposed motion trajectories of the upper platform

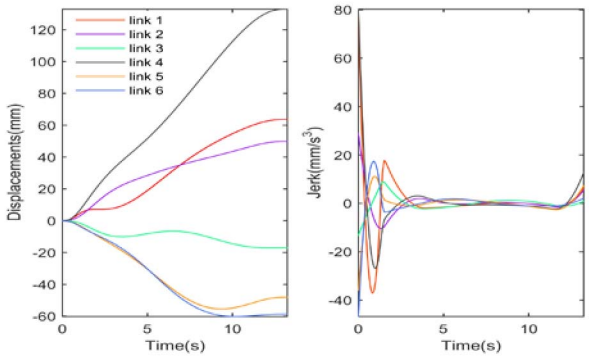


Fig. 7. The minimum time displacement and jerk trajectories of links

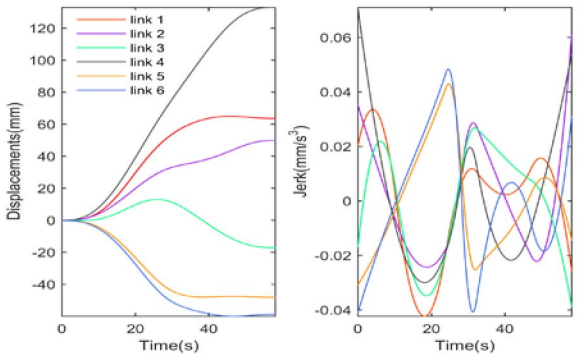


Fig. 8. The minimum jerk displacement and jerk trajectories of links

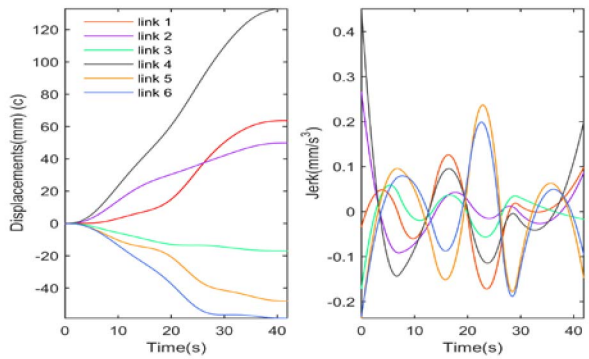


Fig. 9. The minimum energy displacement and jerk trajectories of links

The solutions of Table 3 have indicated that the motion time conflicts with the actuator's jerk. Less motion time leads to higher values of actuators' jerk, but the consumed energy has a relatively stable value, fluctuating around 560J, which does not conflict with the other two objective functions.

The motion trajectoy of the mobile platform have been planned in the workspace, as depicted in Fig.4 and Fig.5, the relative smooth and stable pose trajectories under three objectives have been intuitively represented. The decomposed motion trajectories of the mobile platform have been depicted in Fig.6, which clearly indicate that the minimum motion time trajectory has provided a relatively quicker motion path with 13.23s time spent, the minimum energy trajectory has provided a relatively smaller displacement with 534.98J energy consumed and the minimum jerk trajectory has provided a relatively smoother motion trajectory with a minimum absolute value of 0.07mm/s3.

The displacement and jerk trajectories of actuators have also been obtained via the inverse kinematics model of PAP, as is depicted in Fig.7-9. The displacement and jerk of actuators under three schemes are appropriate for the upper platform with their lower and upper bounds restrained in Table 2. By comparing the jerk curves in Fig.7 and Fig.8, it is obvious that the jerk of actuators fluctuate violently at the initial and final pose in minimum time situation, while the jerk of actuators stay at a smaller and stable value in minimum jerk situation, it proves once again that the motion time conflicts with the actuator's jerk.

## V. CONCLUSION

The proposed trajectory planning scheme is effective for the kinds of 6-DOF parallel manipulators. All the trajectories of the upper platform and the actuated links can be planned and obtained for any two given poses. In this way, the method of trajectory planning for the parallel assembly platform and pose alignment for the large-size components can be achieved.

In the future, further improvement of the performance and computational efficiency of the optimization algorithm will be taken into consideration and more attention will be paid to the trajectory tracking control scheme with different advanced control strategies basing on the planned trajectories.

## REFERENCES


[1] G.Borchert, A.Raatz, "An Analysis Process to Improve the Mobility of a Parallel Robot for Assembly Tasks", in Proc. 14th World Congress in Mechanism and Machine Science, Taipei, 2015.

[2] C. Löchte, F. Dietrich,A.Raatz, "A Parallel Kinematic Concept Targeting at More Accurate Assembly of Aircraft Sections", Intelligent Robotics and Applications, vol. 7101, pp. 142-151, 2011.

[3] B. Dasgupta, T.S. Mruthyunjaya, "The Stewart platform manipulator: a review", Mechanism and machine theory. vol. 35, no. 1, pp.15-40, 2000.

[4] A. Gasparetto, P. Boscariol, A. Lanzutti, R. Vidoni, "Trajectory planning in robotics", Mathematics in Computer Science. vol.6, no. 3, pp. 269-279, 2012.

[5] A. Gasparetto, P. Boscariol, A. Lanzutti, R. Vidoni, "Path planning and trajectory planning algorithms: ageneral overview", in: G. Carbone, F. Gomez-Bravo (Eds.), Motion and Operation Planning of Robotic Systems, vol.29, pp. 3-27, 2015.

[6] C.-T. Chen, T.-T. Liao, "A hybrid strategy for the time-and energy-efficient trajectory planning of parallel platform manipulators", Robotics and Computer-Integrated Manufacturing. vol. 27, no. 1, pp. 72-81, 2011.

[7] C.-T. Chen, H.-V. Pham, "Trajectory planning in parallel kinematic manipulators using a constrained multi-objective evolutionary algorithm", Nonlinear Dynamics. vol. 67, no. 2, pp. 1669-1681, 2012.

[8] E.Yime, R.Saltaren, J. Diaz, "Robust adaptive control of the Stewart-Gough robot in the task space", in Proc. American Control Conference, USA, vol. 58, no. 8, pp. 5248-5253, 2010.

[9] M.R. Azizi, R. Khani, "An algorithm for smooth trajectory planning optimization of isotropic translational parallel manipulators", Proceedings of the Institution of Mechanical Engineers Part C Journal of Mechanical Engineering Science. vol. 230, no. 12, pp. 1987-2002, 2016.

[10] K.C. Tan, C.K. Goh, A.A. Mamun, E.Z. Ei, "An evolutionary artificial immune system for multi-objective optimization", European Journal of Operational Research. vol. 187, no. 2, pp. 371-392, 2008.